

MEASUREMENT OF THE DECAYS  $\psi' \rightarrow \eta J/\psi$  and  $\psi' \rightarrow \pi^0 J/\psi$ \*

M. Oreglia, E. Bloom, F. Bulos, R. Chestnut,  
J. Gaiser, G. Godfrey, C. Kiesling<sup>a</sup>  
Stanford Linear Accelerator Center,  
Stanford University, Stanford, California 94305

R. Partridge, C. Peck, F. Porter  
Physics Department, California Institute of Technology,  
Pasadena, California 91125

W. Kollmann,<sup>b</sup> M. Richardson, K. Strauch, K. Wacker  
Lyman Laboratory of Physics, Harvard University,  
Cambridge, Massachusetts 02138

D. Aschman, T. Burnett,<sup>c</sup> M. Cavalli-Sforza,  
D. Coyne, H. Sadrozinski  
Physics Department, Princeton University,  
Princeton, New Jersey 08540

and

R. Hofstadter, I. Kirkbride, H. Kolanoski,<sup>d</sup>  
A. Liberman,<sup>e</sup> J. O'Reilly, J. Tompkins  
Physics Department and High Energy Physics Laboratory  
Stanford University, Stanford, California 94305

(Submitted to Physical Review Letters)

---

\*Work supported in part by the Department of Energy under contracts DE-AC03-76SF00515 (SLAC), EY-76-C02-3064 (Harvard) and EY-76-C03-0068 (CIT); by the National Science Foundation contracts PHY78-00967 (HEPL), PHY78-07343 (Princeton) and PHY75-22980 (CIT); by the NATO Fellowship, the Chaim Weizmann Fellowship and the Sloan Foundation.

<sup>a</sup>Present address: Max Planck Institute for Physics and Astrophysics,  
Munich, Federal Republic of Germany.

<sup>b</sup>Present address: Wentorfer Strasse 149, 2050 Hamburg, Federal Republic  
of Germany.

<sup>c</sup>Present address: Physics Department, University of Washington,  
Seattle, Washington 98195.

<sup>d</sup>Present address: University of Bonn, Bonn, Federal Republic of Germany.

<sup>e</sup>Present address: Schlumberger-Doll Research Center, Ridgefield,  
Connecticut 06877.

ABSTRACT

The Crystal Ball detector at SPEAR has been used to investigate the decays  $\psi' \rightarrow \eta J/\psi$  and  $\psi' \rightarrow \pi^0 J/\psi$  resulting from production of 776K  $\psi'$ . Our measurement for the branching ratio of the  $\eta$  mode is  $(2.18 \pm 0.14 \pm 0.35)\%$ , where the first error results from statistics and acceptance uncertainties, and the second error is systematic; this is almost a factor of 2 smaller than found in early experiments. For the isospin violating  $\pi^0$  mode we obtain a branching ratio  $(0.09 \pm 0.02 \pm 0.01)\%$ .

We report here a study of 2048 events of the type

$$\psi' \rightarrow \gamma\gamma J/\psi, J/\psi \rightarrow e^+e^- \text{ or } \mu^+\mu^- \quad (1)$$

where for  $\sim 400$  events the photons originate from the decay of an  $\eta$  or a  $\pi^0$ . Detailed consideration of  $\sim 1600$  decays where the photons originate from a cascade through an intermediate  $\chi$  state is left for a future publication. Although the  $\pi^0$  transition may occur electromagnetically, the large branching fraction we observe indicates a breaking of strong isotopic spin symmetry.<sup>1</sup>

Our results are obtained from the examination of  $776\text{K} \pm 78\text{K} \psi'$  (3684) decays, the uncertainty arising from our method for subtracting beam gas background and non-resonant events. The experiment was performed using the Crystal Ball detector at the SPEAR storage ring of the Stanford Linear Accelerator Center. The data were obtained in 4 running periods totaling 6 weeks, which spanned a time of about 5 months. The final data sample resulted from an integrated luminosity of  $1518 \text{ nb}^{-1}$ .

The Crystal Ball detector is a non-magnetic device well suited to the measurement of photons. As shown in figure 1, the detector has as its principal component a 16  $L_{\text{rad}}$  thick, 672 segment shell of NaI(Tl) surrounding cylindrical proportional and magnetostrictive spark chambers. The NaI(Tl) sphere and the inner layer of spark chambers cover 94% of  $4\pi$  sr; the outermost layer of spark chambers covers 71% of  $4\pi$  sr. Endcaps consisting of 60 NaI(Tl) modules (20  $L_{\text{rad}}$  thick) behind magnetostrictive spark chambers supplement the main ball and allow measurements of photons and charged particles over 98% of the  $4\pi$  solid angle. A more complete description of the detector, its electronics, calibration and triggers is published elsewhere.<sup>2</sup>

Hardware energy thresholds were set to allow a >99% trigger efficiency for reaction (1) if all 4 particles had  $|\cos\theta| < 0.9$  ( $\theta$  is the polar angle of the particle with respect to the beam). Monte Carlo calculations using a  $1 + \cos^2\theta$  distribution for the  $\eta(\pi^0)$  show that the resulting geometric acceptance for (1) involving an  $\eta(\pi^0)$  is 0.57(0.50). Acceptances for  $e^+e^-$  and for  $\mu^+\mu^-$  final states differ by less than 0.04; we average the two when quoting acceptances.

The photon and  $e^\pm$  energies were measured in the NaI(Tl), with a resolution  $\sigma = 0.028 \times E^{3/4}$  GeV. Lepton angles were measured with a resolution of  $\sigma = 1^\circ$  using the tracking chambers, except for the 14% of the leptons which had trajectories intersecting only the innermost chambers; in the latter case, the tracks were identified as charged, and angles were determined with a poorer resolution ( $1.5^\circ$  for  $e^\pm$  and  $3.2^\circ$  for  $\mu^\pm$ ) by using the particle's shower energy deposition pattern in the

NaI(Tl). Photon directions were also measured in this manner, but with  $\sigma = 1.5^\circ - 2^\circ$ , depending on the photon energy.

A first selection of event candidates is made by a combination of energy and topology requirements. We require  $E_{\text{event}}$  to be in the range  $3684 \pm 368$  ( $1050 \pm 262$ ) MeV for  $e^+e^-(\mu^+\mu^-)$  final states. Lepton candidates are required to have at least partial tracks in the tracking chambers and a measured energy  $E_e > 900$  MeV for each  $e^\pm$  or  $160 < E_\mu < 280$  MeV for each  $\mu^\pm$ . A muon from (1) has an average deposited energy  $\langle E_\mu \rangle = 210$  MeV; in addition, the energy deposition pattern for muons is quite compact. Therefore we require in  $\mu^\pm$  energy clusters fewer than 5 contiguous NaI(Tl) modules having more than 10 MeV each. Photons are identified as energy clusters with  $E_\gamma$  greater than 20 MeV, having neither a corresponding track nor partial track in the tracking chambers. The calculated neutral energy in (1) lies between the limits of 542 and 589 MeV. We therefore impose the additional criterion of  $E_{\text{neutral}} > 490$  MeV. To further suppress background (mainly the  $\pi^0\pi^0$  background described below) we also require that the endcaps contain less than 8 MeV. The last two cuts result in no additional loss of efficiency for (1).

In order to avoid confusion when shower distributions overlap, we require  $\cos\theta_{ij} < 0.9$ , where  $\theta_{ij}$  is the angle between any two particles  $i$  and  $j$ . In addition, for  $e^+e^-$  final states, all apparent photons with  $20 < E_\gamma < 40$  MeV and  $\cos\theta_{\gamma e} > 0.85$  ( $\theta_{\gamma e}$  is the angle between photon and electron) are taken to be fluctuations in the electron's shower energy pattern; energies of such tracks are added to the electron energy measurement. Monte Carlo studies show that the above energy and overlap cuts reduce the acceptance of the decay involving an  $\eta(\pi^0)$  to 0.47(0.41).

Finally, events are taken to be candidates for (1) only if two photons, each with  $E_\gamma > 40$  MeV, and two leptons are measured in the allowed solid angle of  $|\cos\theta| < 0.9$ . We require that no additional tracks appear elsewhere in the detector. Five percent of the desired decays are lost due to conversion of photons in material before they leave the tracking chambers; four percent are lost due to tracking chamber inefficiency. Photon detection efficiency for  $E_\gamma > 40$  MeV exceeds 99%. Eight percent of the  $\pi^0$  events are lost because of the  $E_\gamma > 40$  MeV requirement; however, the  $\eta$  events are not affected.

The 2225 events satisfying the above requirements are shown on a Dalitz plot, in figure 2a, before kinematic fitting. In addition to the clear  $\eta$  signal,  $\chi(3.51)$  and  $\chi(3.55)$  are evident. A band at the  $\pi^0$  mass is also seen, as well as a general background. Most of the general background is removed by kinematically fitting the events to the hypothesis that they arise from (1). The fits are 5C(3C) for  $e^+e^-(\mu^+\mu^-)$  final states. The confidence level distributions for the fits are flat for both  $e^+e^-$  and  $\mu^+\mu^-$  final states, when a cut at C.L.  $> 0.005$  is made. The remaining 2048 fitted events are shown in figure 2b along with the kinematic limits of the Dalitz plot for our experimental acceptance. Monte Carlo calculations yield an overall detection efficiency for states involving an  $\eta(\pi^0)$  of 0.43(0.35).

Historically, the most serious potential background to (1) resulted from the reaction

$$\psi' \rightarrow \pi^0\pi^0 \text{ J}/\psi, \pi^0 \rightarrow \gamma\gamma \quad (2)$$

when two photons escaped detection. This background is highly suppressed in the Crystal Ball detector due to the large solid angle covered and the ability to measure low energy photons precisely. Monte Carlo simulation of the  $\pi^0\pi^0$  background requires knowledge of the shape of the  $\pi\pi$

mass distribution. We have therefore measured the  $\pi^0\pi^0$  mass distribution, which is shown in figure 3a along with the  $\pi^+\pi^-$  mass distribution obtained recently by the Mark II detector at SPEAR.<sup>3</sup> The shapes of the two distributions are the same within errors, as is expected from isospin symmetry. A Monte Carlo study (using the  $\pi^+\pi^-$  mass distribution measured by the Mark II group and normalized to our data) yields 140 background events before kinematic fitting, none having  $m_{\gamma\gamma}$  less than  $200 \text{ MeV}/c^2$ . Kinematic fitting diminishes the contamination to 7 events, 5 having  $m_{\gamma\gamma} > 525 \text{ MeV}/c^2$ . The Monte Carlo study for  $\pi^0\pi^0$  events has been checked by comparing the number of events it predicts in control regions of the Dalitz plot with those observed, both before and after fitting. A Monte Carlo estimate of the QED process  $e^+e^- \rightarrow e^+e^- \gamma\gamma$  yields fewer than 2 events (after kinematic fitting).

The projection of the Dalitz plot in figure 2b onto the  $m_{\gamma\gamma}$  axis is presented in figure 4a. We separate 412  $\eta$  events from the  $\chi$  and  $\pi^0$  events by requiring  $m_{\gamma\gamma} > 525 \text{ MeV}/c^2$ . This cut removes no  $\eta$  events, but Monte Carlo simulation shows that it admits 21  $\chi(3.51)$  events, as well as the 5  $\pi^0\pi^0$  background events described previously. We subtract these 26 events from the  $\eta$  mass distribution. The remaining 386  $\eta$  events yield a mass  $\langle m \rangle = 547.3 \pm 0.5 \pm 0.9 \text{ MeV}/c^2$ . The first error is statistical and the second is systematic, arising from the uncertainties in the  $J/\psi - \psi'$  mass difference<sup>4</sup> and the non-gaussian energy line shape of NaI(Tl). A width ( $\sigma$ ) of 1.2% for the  $\eta$  signal is consistent with that expected for an  $\eta$  resulting from (1). The detector acceptance has been checked by plotting the energy distribution of photons from the  $\eta$  decay and the polar angle of the reconstructed  $\eta$  (figures 3b and 3c). The resulting distributions are consistent with our Monte Carlo simulation.

After correcting for detection efficiency, acceptance, and the  $\gamma\gamma$  branching fraction of the  $\eta$ , we obtain a value

$$\text{BR}(\psi' \rightarrow \eta J/\psi) = (2.18 \pm 0.14 \pm 0.35)\% .$$

The first error reflects only the statistical error and uncertainty in acceptance, while the second error describes uncertainty in  $\text{BR}(J/\psi \rightarrow e^+e^-)$ <sup>5</sup> and in the number of  $\psi'$ . This branching ratio is considerably smaller than the earlier values of  $(3.5 \pm 0.9)\%$ ,<sup>6</sup>  $(3.6 \pm 0.5)\%$ <sup>7</sup> and  $(4.3 \pm 0.8)\%$ ,<sup>8</sup> but is in good agreement with a new measurement by the Mark II group<sup>9</sup> of  $(2.5 \pm 0.6)\%$ .

A signal at the  $\pi^0$  mass is seen in both the unfitted and fitted Dalitz plots (figure 2a,b). Events containing  $\chi$  states are removed from figure 4a by rejecting events with  $(M_{\gamma-J/\psi})_{\text{high}}$  in the ranges 3405-3415 and 3470-3590  $\text{MeV}/c^2$ , reducing the overall acceptance for  $\pi^0$  events to 0.24. The resulting projection of the Dalitz plot is shown in figure 4b (only events with  $m_{\gamma\gamma} < 525 \text{ MeV}/c^2$  are shown). A gaussian plus quadratic background fit to  $m_{\gamma\gamma}$  yields 23 events above background, at  $\langle m \rangle = 136.1 \pm 2.5 \text{ MeV}/c^2$ , with a width ( $\sigma$ ) of 7.7%, the expected mass resolution for a  $\pi^0$  from (1). The 8 events with  $m_{\gamma\gamma} < 200 \text{ MeV}/c^2$  obtained from the quadratic background are consistent with a Monte Carlo estimate of 5 events from  $\chi(3.41)$  and the tail of  $\chi(3.51)$ . Possible background from continuum production of  $e^+e^- \rightarrow \pi^0 J/\psi$  (an electromagnetic process which does not violate isospin symmetry) has been checked by examining  $1772 \text{ nb}^{-1}$  of data acquired at  $\psi''(3772)$ . Only one event is observed as a possible candidate for  $e^+e^- \rightarrow \pi^0 J/\psi$ ,  $J/\psi \rightarrow e^+e^-$  at  $E_{\text{cm}} = 3772 \text{ MeV}$ ; this gives a 90% C.L. upper limit branching ratio for non-resonant  $e^+e^- \rightarrow \pi^0 J/\psi$  at  $E_{\text{cm}} = 3684 \text{ MeV}$  of 0.01%.<sup>11</sup>

We determine that

$$\text{BR}(\psi' \rightarrow \pi^0 \text{ J}/\psi) = (0.09 \pm 0.02 \pm 0.01)\% .$$

Errors are quoted as in the  $\eta$  result. The Mark II group at SPEAR<sup>9</sup> has obtained a value of  $(0.15 \pm 0.06)\%$ .

We gratefully acknowledge the efforts of A. Baumgarten and J. Broeder of SLAC, and B. Beron, E. B. Hughes and R. Parks of HEPL, Stanford University, as well as those of the LINAC and SPEAR staffs at SLAC. This work was supported by the Department of Energy under contract numbers DE-AC-3-76SF00515 (SLAC), EY-76-CO2-3064 (Harvard) and EY-76-CO3-0068 (CIT), and by the National Science Foundation contracts PHY78-00967 (HEPL), PHY78-07343 (Princeton) and PHY75-22980 (CIT). Support for individuals came from the institutions listed, as well as NATO Fellowship (H.K., Federal Republic of Germany), Chaim Weizmann Fellowship (F.P.) and the Sloan Foundation (T.B.). We thank P. Langacker for discussion of the isospin violating decay mechanisms.



REFERENCES

- a) Present address: Max Planck Institute for Physics and Astrophysics, Munich, Federal Republic of Germany.
  - b) Present address: Wentorfer Strasse 149, 2050 Hamburg, Federal Republic of Germany.
  - c) Present address: Physics Department, University of Washington, Seattle, Washington 98195.
  - d) Present address: University of Bonn, Bonn, Federal Republic of Germany.
  - e) Present address: Schlumberger-Doll Research Center, Ridgefield, Connecticut 06877.
1. G. Segre and J. Weyers, Phys. Lett. 62B, 91 (1976); N. Deshpande and E. Ma, Phys. Lett. 69B, 343 (1977); H. Genz, Lett. Nuovo Cimento 21, 270 (1978); R. Bhandari and L. Wolfenstein, Phys. Rev. D17, 1852 (1978); N. Isgur et al., Phys. Lett. 89B, 79 (1979); P. Langacker, Phys. Lett. 90B, 447 (1980); T. Pham, Ecole Polytechnique preprint PRINT 80-0330 (1980).
  2. R. Partridge et al., Phys. Rev. Lett. 44, 712 (1980); E. D. Bloom, in Proceedings of the XIVth Rencontre de Moriond, Les Arcs, France, edited by J. Tran Than Van (1979); Y. Chan et al., IEEE Transactions on Nuclear Science, Vol. NS-25, No. 1, 333 (1978); I. Kirkbride et al., IEEE Transactions on Nuclear Science, Vol. NS-26, No. 1, 1535 (1979).
  3. T. M. Himel, SLAC Report No. SLAC-223 (Ph.D. thesis) (1979).
  4. V. Luth et al., Phys. Rev. Lett. 35, 1124 (1975); their value for the mass difference is  $588.6 \pm 0.8 \text{ MeV}/c^2$
  5. A. Boyarski et al., Phys. Rev. Lett. 34, 1357 (1975); their value for  $\text{BR}(\psi \rightarrow e^+e^-)$  is  $0.069 \pm 0.009$ .

6. R. Brandelik et al., Nucl. Phys. B160, 426 (1979).
7. W. Bartel et al., Phys. Lett. 79B, 492 (1978).
8. W. Tanenbaum et al., Phys. Rev. Lett. 36, 402 (1976).
9. T. M. Hinel et al., Phys. Rev. Lett. 44, 920 (1980).
10. E. Byckling and K. Kajantie, Particle Kinematics, J. Wiley and Sons, p. 110, New York (1973).
11. This result implies that the continuum process  $e^+e^- \rightarrow \eta J/\psi$  contributes less than  $(0.01 \cdot \frac{m_\pi^2}{m_\eta^2})\%$  to  $BR(\psi' \rightarrow \eta J/\psi)$ .

FIGURE CAPTIONS

1. Schematic diagram of the Crystal Ball detector.
2. Dalitz plot for all events  $\psi' \rightarrow \gamma\gamma J/\psi$ .  $(M_{\gamma- J/\psi})_{\text{high}}$  is the mass recoiling from the lower energy photon. a) Unfitted data satisfying the criteria described in the text. b) Events fitted kinematically to reaction (1). The curve shows the kinematic boundary resulting from our cuts, and the relevant states are indicated.
3. Processes affecting  $\psi' \rightarrow \gamma\gamma J/\psi$ . a) The  $\pi\pi$  mass distribution for  $\psi' \rightarrow \pi\pi J/\psi$ . Open circles denote our measurement of  $\pi^0\pi^0$ , solid circles the Mark II measurement of  $\pi^+\pi^-$ . All distributions are normalized to the same number of events. The dotted curve is a phase space model.<sup>10</sup> b) The distribution of measured gamma energy from  $\psi' \rightarrow \eta J/\psi$ ,  $\eta \rightarrow \gamma\gamma$ . c) Polar angle distribution of the  $\eta$  with respect to the incident electrons. Solid curves in b) and c) are Monte Carlo distributions.
4.  $m_{\gamma\gamma}$  spectrum for  $\psi' \rightarrow \gamma\gamma J/\psi$  (fitted data). a) The Monte Carlo calculated background from (2) (solid line) is shown magnified in amplitude by a factor of 10. b) Events with  $(M_{\gamma- J/\psi})_{\text{high}}$  in the range of  $3530 \pm 60$  and  $3410 \pm 5$  MeV/c<sup>2</sup> and  $m_{\gamma\gamma} > 525$  MeV/c<sup>2</sup> subtracted from a).

# THE CRYSTAL BALL EXPERIMENT

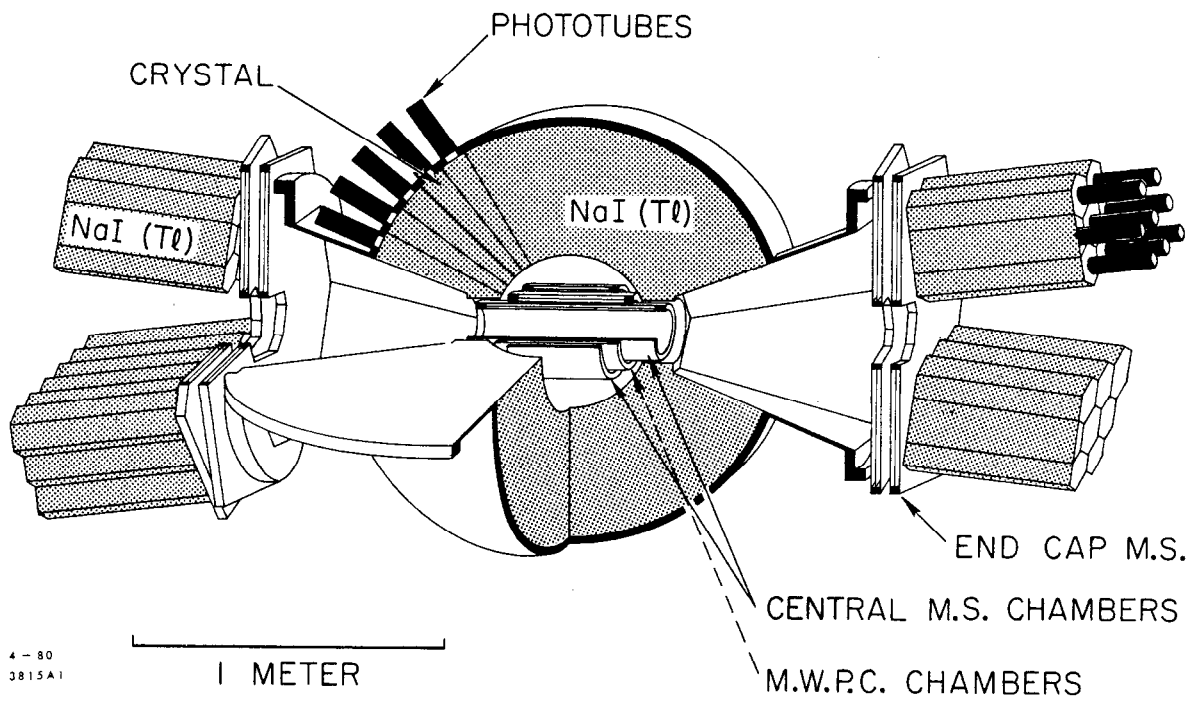


Fig. 1

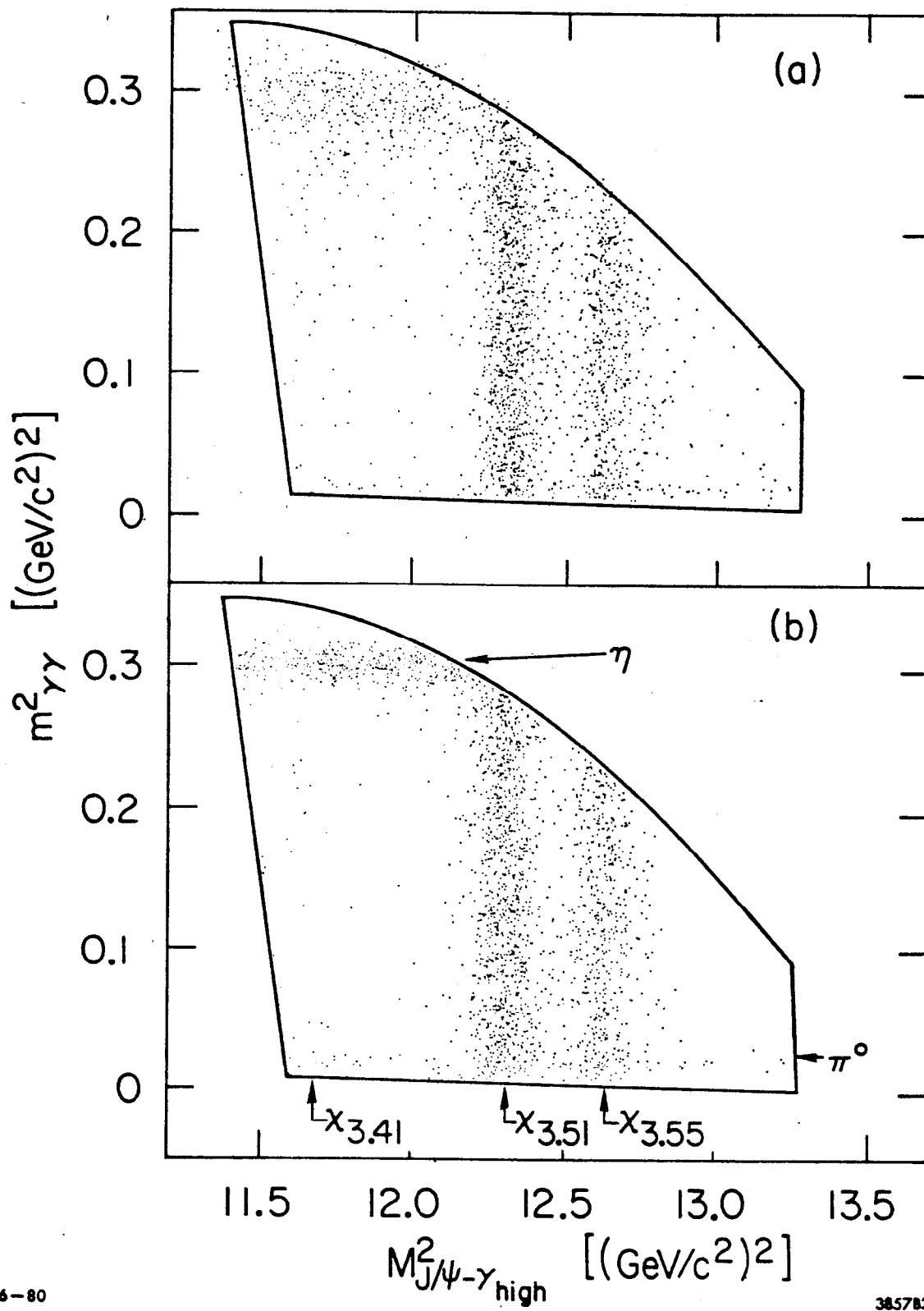


Fig. 2

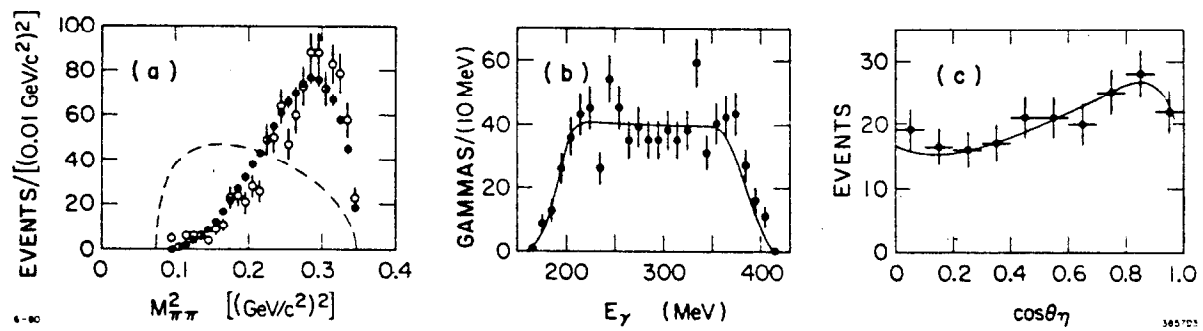


Fig. 3

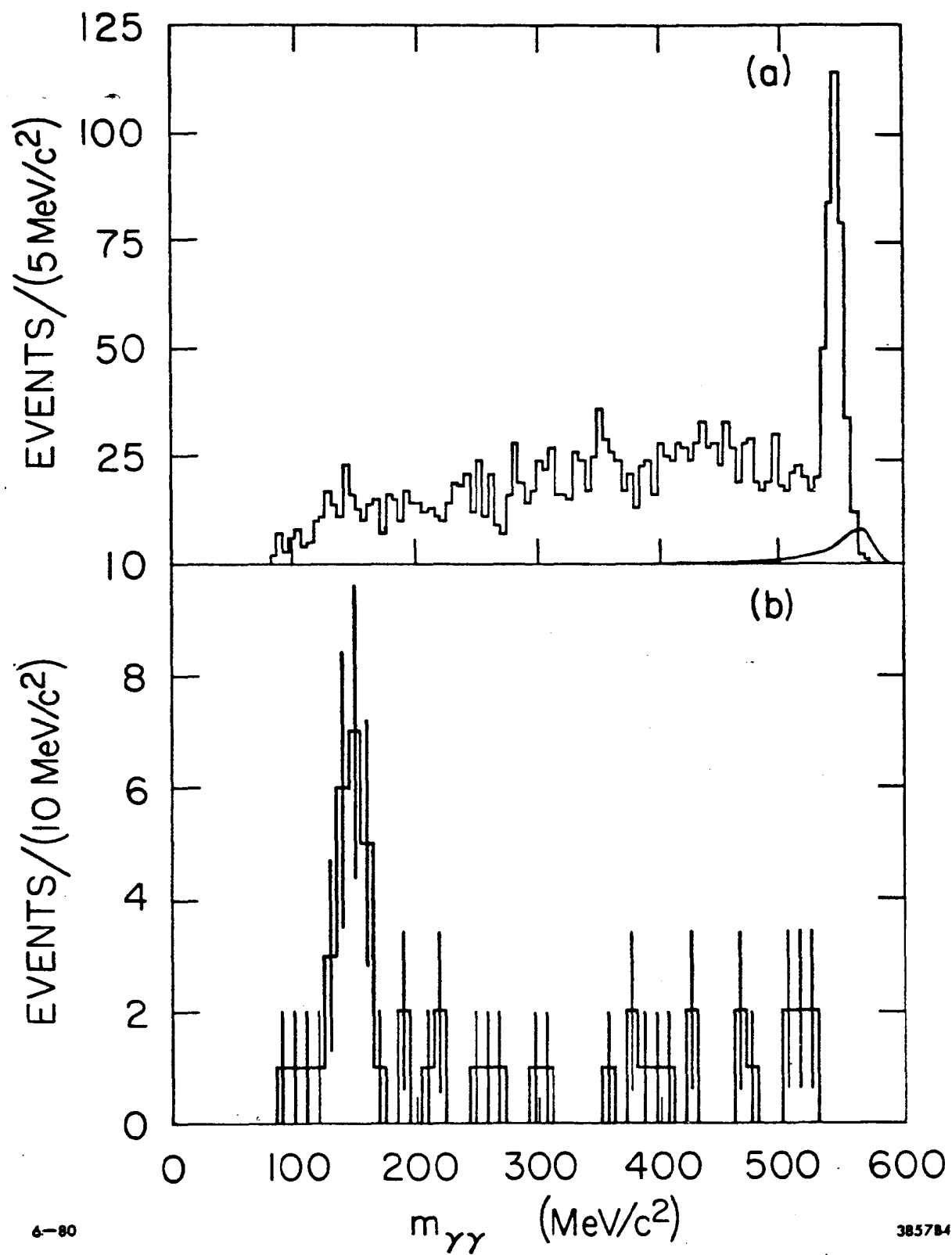


Fig. 4